INFLUENCE OF SUCTION ON SLOPE STABILITY ALONGSIDE THE RIVERBANK

Gerarldo Davin Aventian[1], Alfrendo Satyanaga[2], Robby Yussac Tallar[3], Sung-Woo Moon[2], Jong R. Kim[2]

[1] School of Engineering and Digital Sciences, Nazarbayev University, Astana 010000, Kazakhstan; e-mail: gerarldo.aventian@nu.edu.kz Corresponding author.
[2] School of Engineering and Digital Sciences, Nazarbayev University, Astana 010000, Kazakhstan; e-mail: alfrendo.satyanaga@nu.edu.kz; sung.moon@nu.edu.kz; jong.kim@nu.edu.kz
[3] Department of Civil Engineering, Maranatha Christian University, Bandung 40164, Indonesia; e-mail: robby.yt@eng.maranatha.edu

ABSTRACT
The climatic conditions around the world have recently changed, causing many disasters worldwide, including slope instability. This is a result of the amount of precipitation that damages the slope's safety factor, especially the one that is located near a water reservoir, for instance, a river or a lake. Despite the fact that Kazakhstan is one of the world's permafrost countries that has less precipitation than tropical regions, with approximately 39.000 rivers spread across the nation, many slope failures are possible each year. The main objective is to study the suction effect on slope stability in Kazakhstan. The data were collected from available geotechnical investigations, and numerical analysis were done using SEEP/W and SLOPE/W. To conclude, when compared to the slope model without taking suction into account, the slope model with suction consideration displays a higher factor of safety (FoS).

Keywords: factor of safety, rainfall, soil suction

INTRODUCTION

Slope instability is a recurrent catastrophe that occurred across the globe where it has taken many fatalities and lots of property loss. The World Health Organization estimates that 4.8 million people worldwide have already been impacted by landslides between 1998 and 2017, with more than 18,000 fatalities. Furthermore, according to the United States Geological Survey (USGS), the landslides are believed to be responsible for $1 billion worth of damages and 25 to 50 fatalities annually in the United States alone. One of the causes of this event is the change in rainfall and climate activity, which has affected the stability of the slope since it produces a rise in groundwater table as well as in seawater and river levels.

In riverbank cases, for example, the unstable slopes occur due to several variable, particularly during rainy season, such as change in river water level, pore water pressure, soil strength, and soil erosion (Thi & Minh, 2019). Soil strength is one of the important engineering characteristics that can influence the stability due to the existence of the vadose zone. "Vadose zone" is a term to describe the area above the groundwater level where it is associated with negative pore-water pressure or soil suction. Additionally, soil suction increases the shear strength, supporting the stability of the slope. The decline in soil suction, however, is a result of the river's water level rising. The increased shear strength in the soil is subsequently diminished, which has an impact on the slope's stability and safety factor.

In this study, the results of numerical analyses that were carried out to evaluate the impact of variations both in river water level and rainfall on slope stability are presented. To confirm the correctness of the analyses, numerical calculations were conducted using the limit equilibrium method. In the analysis, several models with varying water tables are employed to determine how safety factor variance varies over time.

LITERATURE REVIEW

Soils in Kazakhstan

The landmass of Kazakhstan has a remarkably diversified soil structure. This is brought on by variations in vegetation, geography, underlying rocks, and climate. Chernozems, chestnut soils, brown and gray-brown soils, which are steppe and desert soils, predominate here as shown in Figure 1 below. Throughout all zones, river valleys frequently have meadow soils, whereas regions with a lot of humidity often have swamp soils (Pachikin et al., 2013; Satyanaga et al., 2022). Expansive soils, which are common in the plains, dry steppes, and semi-deserts, fluctuate in volume in response to variations in water contents. Such soils are widespread in places like Kazakhstan, Egypt, the United States, South Africa, Georgia, Azerbaijan, Ukraine, and Russia. Numerous risks and effects are brought on by expanding soils' harm to buildings, particularly pavements and building foundations. (Pachikin et al., 2013; Satyanaga et al., 2022)

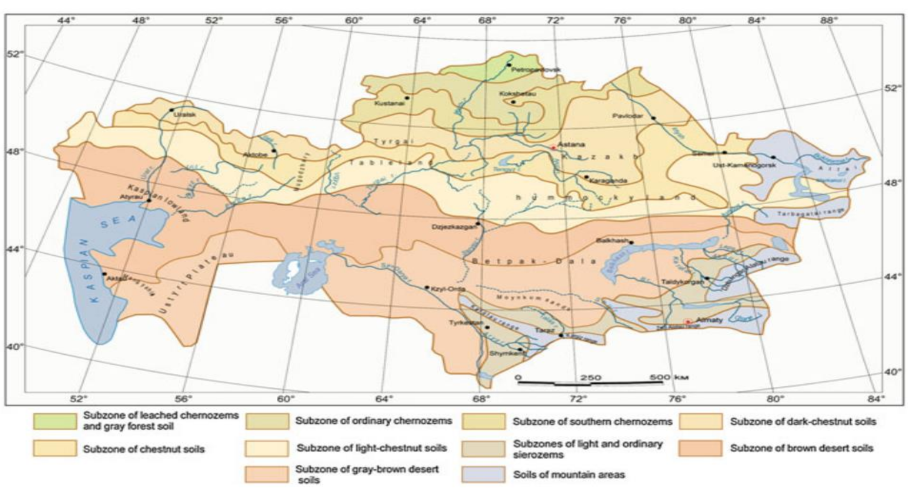

Figure 1. Map of Kazakhstan's soils (Pachikin et al., 2013; Satyanaga et al., 2022)

Mohr-Coulomb Failure

The shear strength of a soil mass is the internal resistance per unit area that the soil mass can offer to resist failure and sliding along any plane inside it (Das, 2010). In 1900, Mohr argued that a material fails due to a crucial mix of normal stress and shearing stress, not just the maximum amount of either normal stress or shear stress. Mohr's equation is then combined with Coulomb's theory of normal stress in 1776 due to the shear stress on the failure plane, which can be roughly represented by a linear function.

$$\tau_f = c + \sigma \tan \phi \quad (1)$$

There is, however, resistance or reaction to, which is provided by a combination of stresses from the solids, known as effective stress (σ'), and from the water in the pores, known as pore-water pressure (u) (Budhu, 2015). This type of stress is usually found in unsaturated soil.

$$\sigma' = \sigma - u_w \quad (2)$$

where τ_f is shear strength, c is cohesion, σ is total stress, σ is total stress, and u_w is pore-water pressure.

Hence, the contact stress between soil solids is not included in this effective stress concept. Instead, it refers to the average stress on a plane via the soil mass. In the effective stress term, there is also (u_a-u_w) concept which is referred as matrix suction. It is a free energy change in a unit volume of water when isothermally transferred from the soil water state to the free water state and is defined at the soil-water-air representative elementary volume (Zhang et al., 2019).

METHODOLOGY

Soil properties

The soil used to calculate the slope stability alongside the riverbank is from Astana, Kazakhstan, with a depth between 0 and 10 meters. The basic properties of the soil are shown in Table 1. Since the soil type is MH which can be concluded as a fine-grained soil, the triaxial with consolidated undrained (CU) approach is preferred for determination of the effective cohesion (c') and effective friction angle (ϕ'). According to Seidmarova, (2008); Zhussupbekov et al. (2017); Satyanaga et al. (2022), the c' is 12 kPa while the ϕ' is 20^o

Table 1. Soil properties (Satyanaga et al., 2022)

Soil classification (USCS)	MH
Void ratio, e_n	0.81
Moisture content, w (%)	28.7
Elastic modulus, E (MPa)	9
Liquid limit, LL (%)	63.0
Plastic limit, PL (%)	36.0

River depth

The river employed in this slope stability investigation is located in Karaganda, Kazakhstan, and has a depth of 5 m, according to Abuduwaili et al. (2019). Due to its proximity to Astana, Karaganda was selected as the location for the slope stability analysis. The depth of the river then varied by one (1) meter from the initial (6 m and 4 m).

Slope geometry

The ratio between horizontal (H) and vertical (V) in the slope is 2:1. Since it generates the steepest angle that a material may be piled at without collapsing or causing the surface material to slide, which is about 30 degrees (U.S. Army Corps of Engineers, 2021). Many riverbank stabilization methods, including bioengineering and more conventional engineered solutions (such as riprap), have a maximum recommended slope of 2H:1V, though maintaining stable riverine slopes benefits from a slope of 3H:1V or lower (U.S. Department of Agriculture, 2019; U.S. Army Corps of Engineers, 2021).

Soil-water characteristic curve (SWCC) measurements

Kazakhstan soil data were used to classify the soil using the USCS classification before the SWCC was determined (Satyanaga et al., 2022). It is feasible to determine which category soils correspond to using Casagrande's plasticity chart and the Unified Soil Classification System. Fredlund & Xing (1994) then improved the equation by adding independent parameters a, n, m, and θs as a result of their collaborative research on discovering the optimal approach for fitting SWCC as shown in Figure 2.

$$\theta = \left[1 - \frac{\ln\left(1+\frac{\psi}{C_r}\right)}{\ln\left(1+\frac{10^6}{C_r}\right)}\right]\left\{\frac{\theta_s}{\left\{\ln\left[e+\frac{\psi}{a}\right]^n\right\}^m}\right\} \qquad (3)$$

where a is a fitting parameter linked to the soil's air entry value, e is the base of the natural logarithm, n is a fitting parameter related to the curve's maximum slope, and m is a fitting parameter connected to the slope's curvature; Cr is correction factor, θ is volumetric water content and ψ is matric suction.

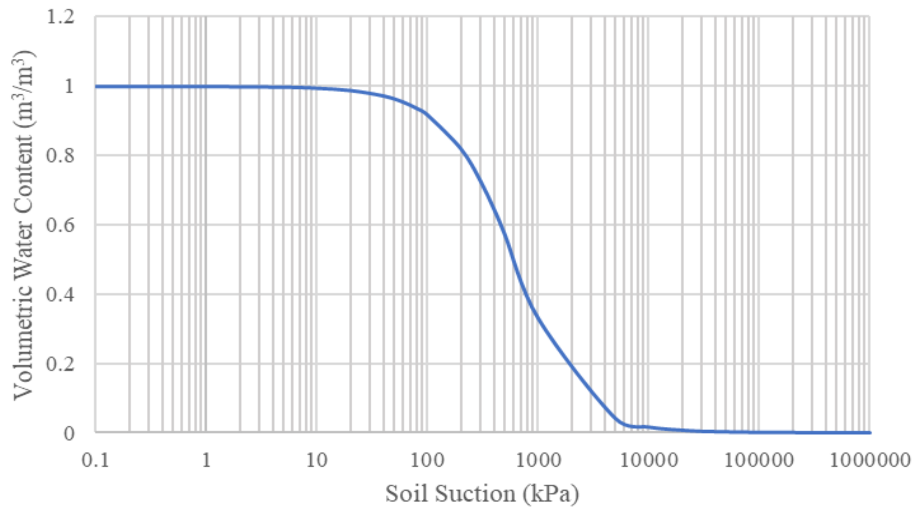

Figure 2. The SWCC of the soil

Permeability function

In an unsaturated soil, both the void ratio and the water content affect the permeability function while on saturated soil, only void ratio that affect the permeability value (Leong & Rahardjo, 1997). The unsaturated permeability calculation (K_w) requires k_s, which is the coefficient permeability of the saturated soil, and it corresponds to SWCC measurement that are fitted using Fredlund & Xing (1994) equation. However, the equation needs to be adjusted with the best fitting parameter for K_w using a, b, c, and p from Leong & Rahardjo (1997) equation. The precision of the statistical model was discovered to be significantly impacted by the quantity and position of discrete points employed in calculation, which in turn depends on how the SWCC is discretized across its whole matric suction range (Zhai & Rahardjo, 2015). The value for each unsaturated permeability function (Figure 3) was then added to the aforementioned software.

$$K_w = \frac{k_s}{\left(\ln \mathrm{e} + \left(\frac{u_a - u_w}{\mathrm{a}}\right)^{\mathrm{b}}\right)^{\mathrm{c\,p}}} \quad (4)$$

where a, n, and m are fitting parameters, and p is a fitting variable ranging from 2.4 to 5.6 for all soil types defined by curve fitting the permeability data. Therefore, the permeability coefficient beyond the residual suction threshold can be assumed to be constant. Because the permeability function above the residual stress condition is more representative of vapor flow (Fredlund et al., 2001).

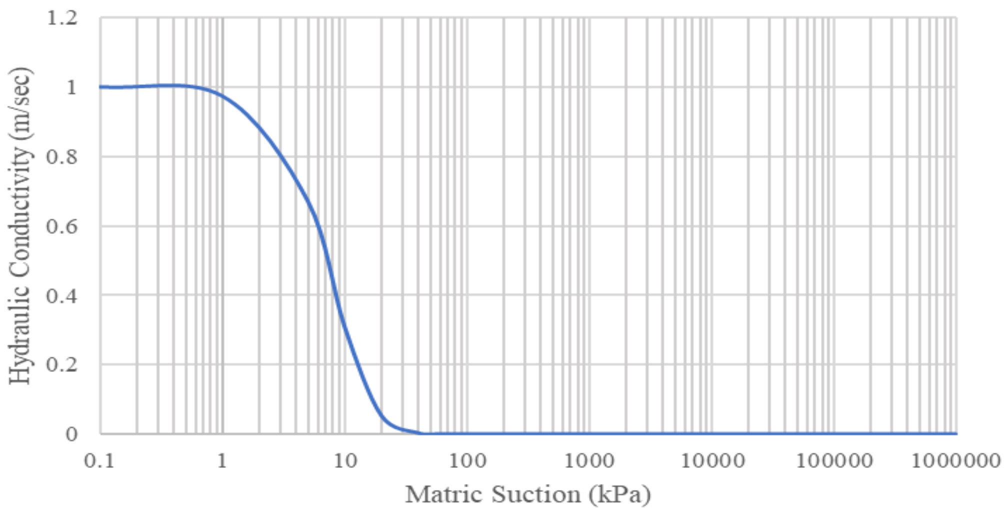

Figure 3. Permeability function graph

Slope Stability Method

Slope stability measurement was executed using SEEP/W combined with SLOPE/W with Morgenstern-Price technique. The Morgenstern-Price method consisted of two factor of safety (FoS) formulas; one for calculating the moment equilibrium while the other one for calculating horizontal force equilibrium (Satyanaga et al., 2022). Although it has stronger equilibrium requirements, this method has grown in favor since it is the most versatile of all methods. Furthermore, the analysis was divided into two (2) parts: one with and one without considering rainfall to analyze the soil suction impact. For the parts that incorporate rainfall, the rainfall was assigned for twelve (12) days using 20 mm/day according to Satyanaga et al. (2022). The stability under dry conditions was determined for another twelve (12) days after the rain conditions had finished.

RESULTS

Pore-water pressure

The representative of pore-water pressure findings from three (3) different groundwater variations which are 4 m, 5 m, and 6 m—are shown in Figure 2. The maximum positive pore pressure in 4m is 220 kPa, while in 5m is 230 kPa and in 6m is 240 kPa. On the contrary, the maximum negative pore pressures in 4 m, 5 m, and 6 m are -50 kPa, -40 kPa, and -30 kPa, respectively. The difference between each variation, both on positive and negative pore-water pressure, is 25%. This is a result of the various groundwater locations; the closer the groundwater table is to the surface, the higher the pore-water pressure that can be developed in the soil's deepest layer. The maximum negative pore-water pressure that was generated can increase the safety factor because it enhances the soil’s strength. From the pore-water pressure results, it can be predicted that the slope with a 4 m groundwater table has the highest soil suction, followed by 5 m depth and 6 m depth.

The contour of pore-water pressure that were generated from seepage analyses of slope with three (3) different groundwater variations can also be seen in Figure 4. The pore-water pressure variations in the soil layers were created due to the rainfall, which has increased the amount of water flowing to the ground. In the slope modeling without rainfall conditions, the pore-water pressure variations in the soil layers are not produced like in Figure 4 because there is no additional water that could be infiltrated. Although the slopes are made of clay soil, which has small pores and thus a low permeability, additional water can still infiltrate through the soil after a certain period of time and reduce the soil's safety factor.

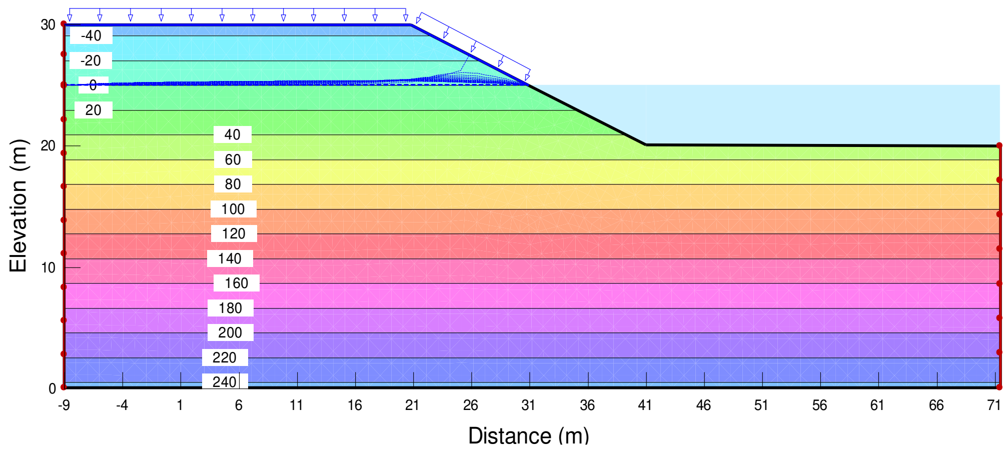

Figure 4. Representative of pore-water pressure result at 5m depth

Factor of Safety (FoS)

The factor of safety variations from three (3) different stability analyses with varying groundwater conditions that are 4m (a), 5m (b), and 6m (c) are shown in Figure 5. The calculation was also performed based on analyses with and without suction to observe the impact of the suction on the slope stability calculation. These graphs demonstrate that the slope model that was given suction at the time of the calculation generated a higher safety factor (SF) than the model without the consideration of soil suction. Furthermore, on a slope model without rainfall conditions, it produces a constant value through the whole time. This is because, in the absence of rainfall situations, the safety factor has been identified at the time the slope is finished. However, in the modeling with rainfall scenarios, the SFs went down after a few days, especially on the fourth (4) day. Consequently, the SF slowly recovered from time to time, especially after the twelve (12) days of rainfall. This is due to the fact that after twelve (12) days of rainfall or wetting treatment, the model has experienced twelve (12) days of drying conditions where there is no additional water left, then the soil suction can aid to regain its SF, even though not to the same extent as in the initial days.

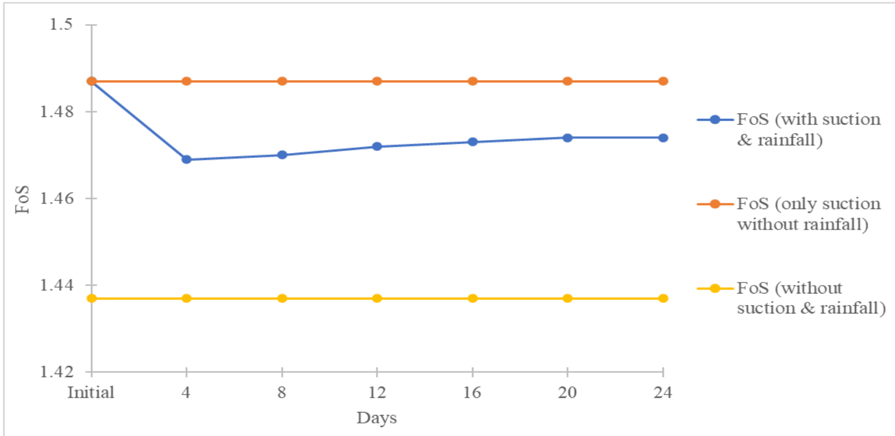

(a) Groundwater table at 4m

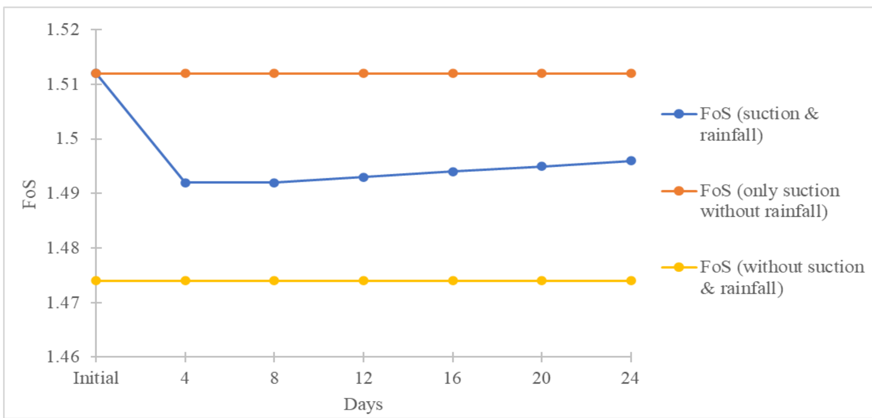

(b) Groundwater table at 5m

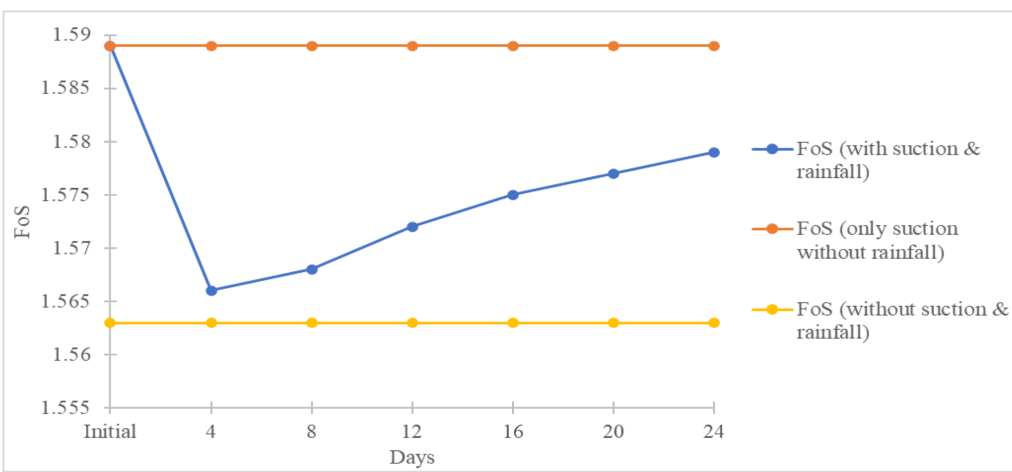

(c) Groundwater table at 6m

Figure 5. Safety factor at different conditions

The initial safety factor results from all of the variations show that the model with a 6 m depth of groundwater has the highest among all. This is because it has the highest groundwater level, which makes the driving force much bigger than the slopes of 4 and 5 meters. In addition, due to the fact that it has the highest groundwater level, the area that has been exposed to rain was much smaller than the others model. Rainfall's impact on the 6 m depth was less significant than it was on the 4 m and 5 m depths.

However, from Figure 5, it is obvious that the slope model with a 6 m depth on the rainfall condition has declined the most after gaining its initial FoS, followed by depths of 5 m and 4 m. As compared to the model's predictions for depths of 4 m and 5 m, the suction effect is less significant at 6 m. The model at 6 m depth, 5 m depth, and 4 m depth has a total decline after an initial FoS of 1.5%, 1.35%, and 1.22%, respectively. This is due to the positive pore-water pressure on the slope at 6 meters being 25% and 50% larger, respectively, than at 5 meters and 4 meters, respectively, of depth.

CONCLUSION

Overall, the study's findings lead to the following conclusions:

1. The slope model with suction consideration possesses a higher factor of safety (FoS) than the slope model without suction consideration.
2. The driving force that generates larger FoS grows with the height of the groundwater table to the surface; however, under rainfall conditions, the FoS on models with higher groundwater tables declines faster than those with lower groundwater levels.

ACKNOWLEDGMENT

This research was supported by Nazarbayev University Research Fund under Grants 11022021CRP1512 and 20122022FD4133. The authors are grateful for this support. Any opinions, findings, and conclusions or recommendations expressed in this material are those of the author(s) and do not necessarily reflect the views of the Nazarbayev University.

REFERENCES

Abuduwaili, J., Issanova, G., & Saparov, G. (2019). *Hydrology and Limnology of Central Asia*. http://www.springer.com/series/7009

Budhu, M. (2015). *Soil Mechanics Fundamental* (1st ed.). John Wiley & Sons, Ltd.

Das, B. M. (2010). Principles of Geotechnical Engineering. In *Journal of Chemical Information and Modeling* (7th ed., Issue 9). Cengage Learning.

Fredlund, D. G., & Anqing Xing. (1994). Equations for the soil-water characteristic curve. *Canadian Geotechnical Journal*, *31*(4), 521–532. https://doi.org/10.1139/T94-061

Fredlund, D. G., Rahardjo, H., Leong, E. C., & Ng, C. W. W. (2001). Suggestions and recommendations for the interpretation of soil-water characteristic curves. *14th Southeast Asian Geotechnical Conference*, 508.

Leong, E. C., & Rahardjo, H. (1997). Permeability Functions for Unsaturated Soils. *Journal of Geotechnical and Geoenvironmental Engineering*, *123*(12), 1118–1126. https://doi.org/10.1061/(ASCE)1090-0241(1997)123:12(1118)

Mississippi Watershed Management Organization. (2010). *A Guide to Bank Restoration Options for Large River Systems: Part II Bioengineering Installation Manual MWMO Watershed Bulletin: 2010-3 Prepared for the MWMO by: Great River Greening*. www.mwmo.org

Pachikin, K., Erokhina, O., & Funakawa, S. (2013). Soils of Kazakhstan, Their Distribution and Mapping. *Environmental Science and Engineering*, 519–533. https://doi.org/10.1007/978-3-319-01017-5_32/COVER

Satyanaga A., Ibrahimi, A. B., Mohammad, A. S., Hamdany, A. H., Wijaya, M., Moon, S.-W., & Kim, J. (2022). Water Characteristic Curve for Soils in Kazakhstan. *Geotechnical Engineering Journal of the SEAGS & AGSSEA* , *53*(4), 1–8. http://seags.ait.asia/seags-agssea-journal-2020-2022-issues/water-characteristic-curve-for-soils-in-kazakhstan/

Satyanaga, A., Moon, S.-W., Kim, J. R. (2022). Stability analyses of dual porosity soil slope. *Geomechanics and Engineering*, *28*(1), 077. https://doi.org/10.12989/GAE.2021.28.1.077

Seidmarova, T. (2008). Investigation of soil characteristics and load-displacement curve of driven piles in loam and clay ground in Astana, Kazakhstan. *6th Asian Young Geotechnical Engineers Conference (AYGEC).*, 164–173.

Thi, T. D., & Minh, D. do. (2019). Riverbank stability assessment under river water level changes and hydraulic erosion. *Water*, *11*(12), 1–20. https://doi.org/10.3390/w11122598

United States Geological Survey. (n.d.). *Landslides 101*. Retrieved October 10, 2022, from https://www.usgs.gov/programs/landslide-hazards/landslides-101

U.S. Army Corps of Engineers. (2021). *Riverbank Stability Assessment and Applied Best Practices Guide Executive Summary*. https://pittsburghpa.gov/innovation-performance/interactive-maps.

U.S. Department of Agriculture. (2019). *Web Soil Survey - Home*. https://websoilsurvey.sc.egov.usda.gov/App/HomePage.htm

World Health Organization. (n.d.). *Landslides*. Retrieved October 10, 2022, from https://www.who.int/health-topics/landslides#tab=tab_1

Zhai, Q., & Rahardjo, H. (2015). Estimation of permeability function from the soil–water characteristic curve. *Engineering Geology*, *199*, 148–156.

Zhang, C., Asce, A. M., Lu, N., & Asce, F. (2019). Unitary Definition of Matric Suction. *Journal of Geotechnical and Geoenvironmental Engineering*, *145*(2). https://doi.org/10.1061/(ASCE)GT.1943-5606.0002004

Zhussupbekov, A., Zhussupbekov, A. Z., Shakhmov, Z. A., Tleulenova, G. T., & Akhazhanov, S. B. (2017). Use of dynamic and static load piling tests in Astana, Kazakhstan. *Industrial Machine Building*, *2*(49), 32–37. https://doi.org/10.26906/znp.2017.49.819